Proc. VI Int. Conf. Borate Glasses, Himeji, Japan, 18–22 August 2008 *Phys. Chem. Glasses: Eur. J. Glass Sci. Technol. B*, October 2009, **50** (5), 284–288

First principle simulations of liquid and vitreous B_2S_3

G. Ferlat[1,*] *& M. Micoulaut*[2]

[1] *Institut de Minéralogie et de Physique des Milieux Condensés, UMR CNRS–IPGP–Universités Paris 6 et 7 no. 7590, 4 place Jussieu, 75252 Paris cedex 05, France*

[2] *Laboratoire de Physique Théorique de la Matière Condensée, Boîte 121, Université Paris 6, 4 place Jussieu, 75252 Paris cedex 05, France*

Manuscript received 27 August 2008
Revised version received 24 April 2009
Accepted 21 July 2009

This paper is part of an ongoing effort aimed at modelling the structure of liquid and vitreous B_2S_3 within a first principles framework. Using density functional theory, finite basis sets and pseudopotentials, we carried out molecular dynamics of the liquid phase. We report tests regarding some of the description parameters, such as the basis and the system size. Preliminary results obtained in the vitreous phase are also presented.

1. Introduction

Thioborate (i.e. B_2S_3 based) compounds have interesting technological applications, for instance as superionic conducting materials for batteries or fuel cells.(1) They are also of fundamental interest as prototypical III–VI network glasses, like B_2O_3 compounds for which they provide comparative insight concerning the structural chemistry.

From a microscopic point of view, it is well established that the molecular building block in both crystalline and glassy B_2S_3 is the planar BS_3 unit. In the B_2S_3-I crystal, these units connect into 4-fold (B_2S_4) and 6-fold (B_3S_6) rings, and there are no independent BS_3 triangles.(2) The 6-fold rings, called borsulphols or thioboroxols, are the equivalent of the boroxol rings in vitreous B_2O_3, while the 4-fold (edge sharing) rings are not observed in borates and are specific to chalcogenides. In the following, we shall refer to f_∞, f_4 and f_6, the relative proportions of boron atoms involved in independent BS_3 triangles, 4- and 6-fold rings, respectively. In B_2S_3-I, f_∞=0, f_4=25 and f_6=75%.

These quantities in the vitreous phase v-B_2S_3 are still uncertain and the information available in the literature is contradictory.(3–11) Support for the existence of both 4- and 6-fold rings, and thus for structural similarities between the glass and the crystal, was inferred from the first Raman studies(3,4) and from NMR data.(5) However, at least in the latter case, contamination of the samples was noticed.(5) More recently, Raman,(6) infrared(7) and diffraction(8,9) studies found no evidence for 4-fold rings, and instead show the glass to be predominantly made of BS_3 triangles and B_3S_6 thioboroxols. In this latter model, v-B_2S_3 would be isostructural to its oxide analogue, v-B_2O_3 for which f_∞~25 and f_6~75%.(12) In a theoretical aggregation model,(10) the B_3S_6 units were found to be energetically favoured over the B_2S_4 rings. Finally, a previous molecular dynamics (MD) simulation using empirical force fields led to a model made almost entirely of chains of B_2S_4 rings (f_4~100%).(11) We note that at the time of this theoretical work(11) the experimental static structure factor of pure v-B_2S_3 was not available, since it was measured only recently.(8) The comparison of the calculated(11) and experimental(8) neutron structure factors clearly allows us to rule out the f_4~100% model (see Figure 5(c) later).

In order to clarify the situation, it is clear that a model which simultaneously reproduces all the mentioned information (diffraction, IR, Raman, NMR) is highly desirable. These considerations motivated us to undertake an extensive description of B_2S_3 disordered phases within a first principles scheme. The purpose of the present work is to assess the validity of our approach and to present preliminary results.

2. Method

2.1 Details of calculations

First principles molecular dynamics (FPMD) simulations were performed within the density functional theory (DFT) framework using generalised gradient approximations (GGA) to the exchange-correlation functional and norm-conserving Troullier–Martins pseudopotentials(13) in the Kleinman–Bylander(14) form. We tested two different GGA functionals, namely PBE(15) and BLYP.(15–17) The core radii used are summarised in Table 1. We used both the CPMD(18) and Siesta(19,20) codes. In the former case, an accurate

Table 1. Core radii used in the Troullier–Martins pseudopotentials for the s, p, d channels depending on the exchange-correlation functional used (PBE(15) or BLYP(16,17))

	r^{B}_{core} (a.u.)			r^{S}_{core} (a.u.)		
	s	*p*	*d*	*s*	*p*	*d*
PBE	1·7	1·7	1·7	1·4	1·4	1·7
BLYP	1·4	1·5	0·9	1·4	1·4	0·95

---

*Corresponding author. Email Guillaume.Ferlat@impmc.jussieu.fr and easy-to-converge plane-wave (PW) basis set is used for the electronic wave functions expansion, rendering however, the simulations very time expensive for large systems. A cut off of 40 Ry was chosen for the PW kinetic energy. In the latter case, the basis set is a combination of localised pseudoatomic orbitals, allowing for a very efficient resolution of the Kohn–Sham equations. It is thus very adapted to simulations of disordered systems, for which large unit cells are required, but the size and shape of the basis set require to be tuned and the accuracy of the results to be checked. We used a double-ζ polarised (DZP) basis set, which amounts to two 2s, two 2p and one 3d shells for both sulphur and boron atoms. The shape and cutoff radii (r_c) of the support regions of the wave functions were obtained variationally(21,20) in a reference system, $B_3S_6H_3$, i.e. a borsulphol molecule with hydrogens terminating the nonbridging sulphurs. A similar procedure was used for our previous simulations of B_2O_3(22,12,23) and a more detailed description can be found in Ref. 22. This resulted in r_c values for the first-ζ of 6·6, 7·3 and 3·7 a.u., respectively, for the s, p, d orbitals of sulphur, and 4·7, 5·2, 4·8 a.u. for boron. In the following, this basis is referred to as DZP-opt. For Siesta calculations, the real-space integrations were carried out on a grid whose fineness is defined by a 250 Ry energy cutoff. This allowed the total force modulus to converge below 0·1 eV/Å at each MD step.

All the simulations were carried out within the Born–Oppenheimer approximation, using an ionic time step of 1 fs, except in simulation #5 (see Table 2) for which the Car–Parrinello method was used with a fictitious electron mass of μ_0=600 a.u. and a time step of 0·1 fs. All the trajectories were sampled at fixed density using NVT or NVE ensembles. The initial configurations were generated from snapshots taken from our previous B_2O_3 simulations.(12) The oxygens were substituted by sulphurs and the cell lattice rescaled so as to get the B_2S_3 glass density, ρ~1·7 g cm^{-3}. We used two different initial configurations taken from either our boroxol-rich (BR) or boroxol-poor (BP) B_2O_3 glasses. The BR (f_6=75%) configuration contains 80 atoms in a monoclinic (almost hexagonal) box, while the BP (f_6=22%) configuration contains 100 atoms in a cubic box. We also generated a larger system of 320 atoms by using a 2×2×1 supercell (almost cubic) of the 80 atoms configuration. γ-point sampling only was used for all the calculations.

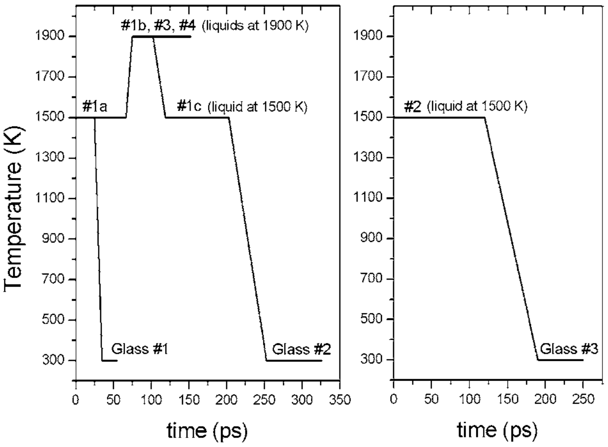

Figure 1. Schematic protocol of the liquid and glass simulations (see Tables 2 and 3)

Table 2 and 3 summarise the characteristics of the liquid and glassy simulations undertaken: basis set, exchange-correlation functional, initial configuration, system size, temperature and duration. Figure 1 shows schematically the protocol used for the thermal sampling, detailed in the next subsection.

2.2 Simulation protocol

We started simulations #1 and #2 (using PW and DZP-opt basis sets respectively) at 1500 K using the BR model as a starting configuration. This model appeared to be quite stable at this temperature; very long times (>50 ps) were required for the system to gradually melt. The melting was monitored from the evolution of the mean squared displacement (MSD). Only simulation #2 was run for a time long enough for the system to melt; in simulation #1a, the system is a hot glass, i.e. only local rearrangements have occurred due to the limited simulation time. Simulations using the BP model (#5) did not show such metastable behaviour; the diffusive regime was quickly reached. Thus, the temperature in simulation #1 was increased to a higher temperature, 1900 K and run for 75 ps (#1b), in order for the system to reach an equilibrium independent of the initial configuration. Simulations at 1900 K using the DZP-opt basis were started from the configuration obtained in #1b after 25 ps: one using the same number of atoms (#3) was run for 50 ps, another one using 320 atoms for 12 ps

Table 2. Parameters describing the high temperature simulations: PW stands for plane wave basis sets using a 40 Ry cutoff and the CPMD code, DZP-opt. stands for the optimised double-ζ polarised basis using Siesta, XC is the exchange-correlation functional (PBE(15) or BLYP(16,17)), and finally BR and BP stand for boroxol-rich and boroxol-poor respectively (see text)

	Basis set	*XC*	*Initial configuration*	T *(K)*	*Duration (ps)*
#1a	PW	PBE	BR (80 atoms)	1500	65
#1b	PW	PBE	continuation from #1a	1900	75
#1c	PW	PBE	branched from #1b	Quench -1500	16 + 84
#2	DZP-opt.	PBE	BR (80 atoms)	1500	120
#3	DZP-opt.	PBE	started from #1b, 80 atoms	1900	50
#4	DZP-opt.	PBE	started from #1b, 320 atoms	1900	12
#5	PW	BLYP	BP (100 atoms)	1500	35

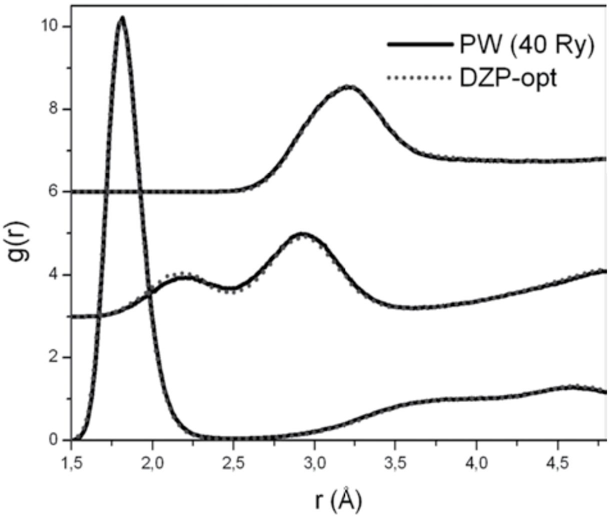

Figure 2. From bottom to top: B–S, B–B and S–S partial pair correlation functions obtained from simulations #1b and #3 (see Table 2)

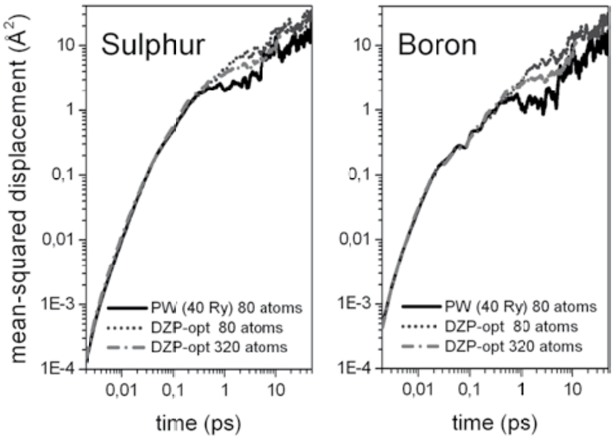

Figure 3. Mean squared displacements of sulphur (left) and boron (right) atoms at 1900 K as a function of time in simulations #1b, #3 and #4 (see Table 2)

(#4). Finally, a quench at 1500 K was branched from simulation #1b for a duration of 16 ps ($2{\cdot}5\times10^{13}$ K/s) and the liquid at 1500 K was sampled for 86 ps.

In the following section, the simulations carried out at 1900 K (#1b,#3, #4) are used to compare the calculation methodologies (basis and system sizes), since this temperature appeared to be high enough to reach the diffusive regime and thus an equilibrium independent from the initial configuration. On the contrary, simulations carried out at 1500 K (#1a, #1c, #2, #5) do show dependencies on the thermal history (due to the limited simulation times) and we shall use this dependency to generate several glassy models.

The first glass was obtained from a quench to 300 K branched from simulation #1a: this glass (G1) is fully isostructural to the starting configuration, i.e. the boroxol-rich model of B_2O_3. The second glass (G2) was obtained from a quench initiated from simulation #1c (quenched at $2{\cdot}5\times10^{13}$ K/s over 50 ps and then relaxed at 300 K for 70 ps); its thermal history thus includes the high temperature (1900 K) liquid state. Finally, the third glass (G3) was obtained from simulation #2 (quenched at $1{\cdot}7\times10^{13}$ K/s over 70 ps and then relaxed at 300 K for 60 ps).

3. Results

Figure 2 compares the partial pair correlation functions (PPCFs), calculated for the same duration (50 ps) at 1900 K from simulations #1b and #3, thus allowing to probe the effects of the basis size. The B–S and S–S curves are almost identical while very small differences are visible in the B–B PPCF, in particular the height and shape of the first B–B peak at ~2·1 Å. These differences are, however, marginal; the integration of the B–B PPCF up to the first minimum (2·45 Å) gives n_{BB} (B–B coordination number) values of 0·47 and 0·50 for simulations #1b and #3, respectively. The same is true for the angular distributions (not shown); small or no differences at all were observed between both simulations. A more stringent test is provided by the dynamics; we monitored the MSD and the fraction of rings as a function of the simulation time. Both quantities showed a very similar behaviour in either type of simulation, see Figure 3.

Figure 4 compares again the PPCF obtained at 1900 K from simulations #3 and #4, thus allowing to probe system size effects. Although not fully negligible, the differences are rather small, the most important being found again in the first B–B peak (n_{BB} values of 0·50 and 0·40 were obtained). The dynamics were found to be unaffected by the system size within the statistical uncertainties (Figure 3). Longer simulations, however, are required for a more definitive assessment.

The comparison of the results from simulations #1c and #5 allows to probe primarily the effect of the XC functional; the obtained PPCFs (not shown) were found to be essentially the same with, however, a slight shift of the first peak position to higher r, by approximately 0·01–0·03 Å in the BLYP case as compared to the PBE results. Since there are no experimental data available for the liquid, it is not possible yet to favour one or the other of these two functions. However, this choice does not seem to be critical.

The fraction of n-fold rings has been calculated for each liquid snapshot, and averaged over all snapshots. The results for the liquids at 1500 K are

Table 3. Parameters describing the obtained glassy models (using the same notation as in Table 2)

Glass	*Basis set*	*XC*	*Initial configuration*	T *(K)*	*Duration (ps)*
G1	PW	PBE	branched from #1a (after 25 ps)	Quench - 300	10 + 20
G2	PW	PBE	branched from #1c (after 200 ps)	Quench - 300	50 + 70
G3	DZP-opt.	PBE	branched from #2 (after 120 ps)	Quench - 300	70 + 60

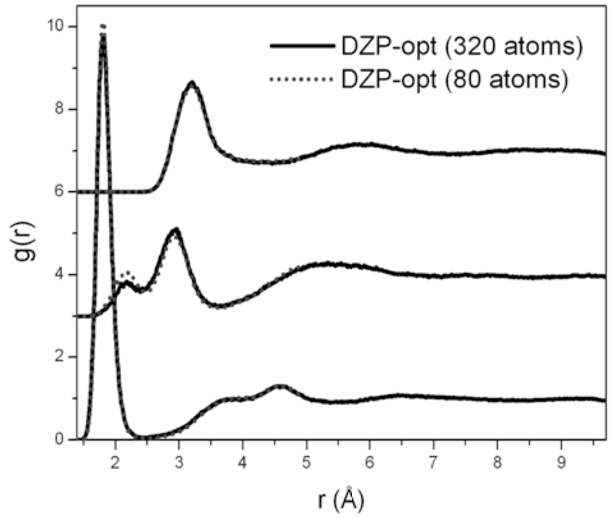

Figure 4. From bottom to top: B–S, B–B and S–S partial pair correlation functions obtained from simulations #3 and #4 (see Table 2)

presented in Table 4. Due to the limitations in both simulation times and system sizes, an error bar of at least 5 % should be assigned to these averaged values.

Table 4. Average relative proportion (in %) of boron atoms in independent triangles (f_∞), 4-fold (f_4) and 6-fold (f_6) rings in the liquid samples at 1500 K

Simulation	f_∞	f_4	f_6
#1c	14	28	58
#2	19	16	65
#5	7	37	56

4. Discussion

The structural and dynamic quantities explored in our liquid simulations showed no or weak dependencies upon the methodology used. In particular, the system description is not degraded by the use of the localised basis set (in simulations #2, #3, #4) as compared to the more expensive PW basis set (Figures 2 and 3). Moreover, finite system size effects are minor (Figures 3 and 4), at least in the range explored (from 80 to 320 atoms). It is quite reassuring that, despite the differences in methodologies and/or thermal histories used in the liquid simulations at 1500 K (#1c, #2 and #5), the average ring statistics (Table 4) is qualitatively the same in all three samples (Table 4); the liquid at 1500 K is predominantly made of 6-fold rings (~60%) with, however, a significant amount of 4-fold rings (~10–40%).

The presence of 4-fold rings in the liquid is likely a robust result; though they were absent from all of the initial configurations, their occurrence is a systematic output for long enough simulations, from values of ~10 to ~40%. The predominance of borsulphol rings at 1500 K is also strongly supported by the simulations; independently of the initial value (22% in simulation #5, 75% in the others), an equilibrium around 60±10% was observed. The determination of the ring statistics in the glassy state is more problematic due to the use of quenching rates which are much too fast; the obtained glass is in general strongly reminiscent of the liquid configuration from which the quench was initiated. Our strategy is thus to use the dependency of the glass structure upon its thermal history to generate several numerical glassy models. These models will then be compared with the available

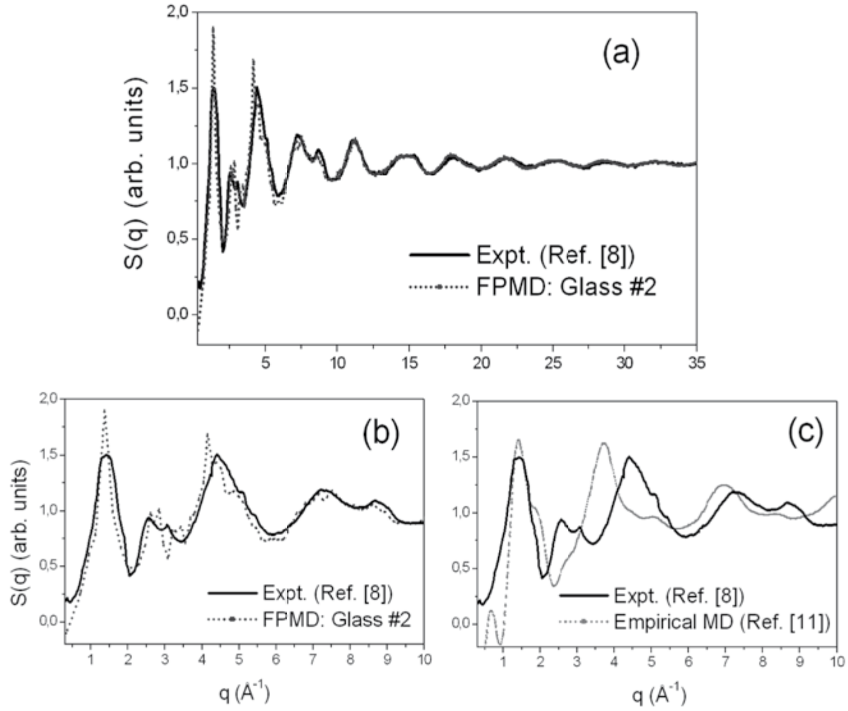

Figure 5. (a) calculated (dots) and experimental[(8)] (solid line) neutron weighted total static structure factor at 300 K, (b) the same data, expanded in the 0–10 Å^{-1} range, and (c) results from a previous empirical MD study[(11)]

Table 5. Relative proportion (in %) of boron atoms in non-ring units (f_∞)*, 4-fold* (f_4)*and 6-fold* (f_6) *rings in the glassy samples*

Glass	f_∞	f_4	f_6
G1	25	0	75
G2	0	44	56
G3	22	12	66

experimental information (diffraction, infrared, Raman and NMR).

We generated three different glasses (see Table 3) for which the ring statistics noticeably differ (Table 5), thus allowing us to test different hypotheses proposed for v-B_2S_3. If the glass structure is close to that of the liquid obtained at 1500 K, then the G2 model should be the most realistic. We note that the numbers obtained for this model are pretty similar to those of the known crystal. On the contrary, if 4-fold rings do not survive in the glass, then the G1 model, isostructural to v-B_2O_3 should be closer to reality. The G3 model is somehow intermediate between G1 and G2.

As a first test, Figure 5(a) compares the neutron weighted total static structure factor calculated for the G2 glass to the experimental data.(8) The agreement is overall very good, even in the region of the first sharp diffraction peak (Figure 5(b)). Within the statistical uncertainty, a similar level of agreement was obtained for all of our three glasses (not shown), in spite of significant differences in the model B–B PPCFs; this is due to the fact that the total structure factor is dominated by the B–S partial contribution. Unfortunately, there are as yet no experimental partial structure factors available. However, the disagreement is obvious in the case of the chain of 4-fold rings model, formerly obtained from classical MD(11) (Figure 5(c)). This illustrates both the higher degree of realism of the first-principles models provided in this work, and the rather poor sensitivity of the total structure factor to the details of the ring statistics. As found in the case of B_2O_3,(12) the reproduction of the total structure factor is a necessary condition, but not a sufficient one.

To gain further insight, we plan to compute Raman, infrared and ^{11}B MQMAS (multiple quantum magic-angle spinning) spectra, which constitute much more stringent tests of the models.(12)

5. Conclusions

First-principle molecular dynamics simulations of liquid and vitreous B_2S_3 have been carried out. It has been shown that results of comparable accuracy to PW ones can be obtained with rather small basis (DZP like), making the extension of simulation times and/or system sizes affordable. Simulations of the liquid at 1500 K show the presence of large amounts of both 4- and 6-fold rings. Several glassy models, differing by their amount of 4- and 6-fold rings, have been generated by varying the thermal history. The obtained models are all consistent with neutron diffraction experiments, which is not the case of the numerical model proposed formerly in the literature.(11) To quantify more precisely the amount of rings in the glass, we shall compare the predictions of our models with the results of spectroscopic probes (infrared, Raman and NMR), which may allow us to discriminate between them.

Acknowledgements

We thank A. P. Seitsonen and C. Massobrio for providing us with some of the pseudopotentials, and A. Takada for providing us with the initial B_2O_3 BR (boroxol-rich) configuration. The calculations have been performed at the French supercomputing centres IDRIS, CINES and CCR. G. Ferlat acknowledges financial support from IUCr2008 for attending the Borate2008 conference.

References

1. Kincs, J. & Martin, S. W. *Phys. Rev. Lett.*, 1996, **76**, 70.
2. Diercks, H. & Krebs, B. *Angew. Chem.*, 1977, **89**, 327.
3. Geissberger, A. E. & Galeener, F. L. In: *The structure of non-crystalline materials*, Eds. P. H. Gaskell, J. M. Parker & E. A. Davis, Taylor and Francis, London, 1983, p. 381.
4. Menetrier, M., Hojjaaji, A., Levasseur, A., Couzi, M. & Rao, K. J. *Phys. Chem. Glasses*, 1992, **33**, 222.
5. Hwang, S.-J., Fernandez, C., Amoureux, J., Han, J.-W., Cho, J., Martin, S. W. & Pruski, M. *J. Am. Chem. Soc.*, 1998, **120**, 7337.
6. Royle, M., Cho, J. & Martin, S. W. *J. Non-Cryst. Solids*, 2001, **279**, 97.
7. Cho, J. & Martin, S. W. *J. Non-Cryst. Solids*, 1995, **182**, 248.
8. Sinclair, R. N., Stone, C. E., Wright, A. C., Martin, S. W., Royle, M. L. & Hannon, A. C. *J. Non-Cryst. Solids*, 2001, **293**, 383.
9. Yao, W., Martin, S. W. & Petkov, V. *J. Non-Cryst. Solids*, 2005, **351**, 1995.
10. Micoulaut, M. In: *Current problems in condensed matter*, Ed. J. L. Morán-López, Plenum Press, 1998, p. 339.
11. Balasubramanian, S. & Rao, K. J. *J. Phys. Chem.*, 1994, **98**, 9216.
12. Ferlat, G., Charpentier, T., Seitsonen, A. P., Takada, A., Lazzeri, M., Cormier, L., Calas, G. & Mauri, F. *Phys. Rev. Lett.*, 2008, **101**, 065504.
13. Troullier, N. & Martins, J. L. *Phys. Rev. B*, 1991, **43**, 1993.
14. Kleinman, L. & Bylander, D. M. *Phys. Rev. Lett.*, 1982, **48**, 1425.
15. Perdew, J. P., Burke, K. & Ernzerhof, M. *Phys. Rev. Lett.*, 1996, **77**, 3865.
16. Becke, A. D. *Phys. Rev. A*, 1988, **38**, 3098.
17. Lee, C., Yang, W. & Parr, R. G. *Phys. Rev. B*, 1988, **37**, 785.
18. Copyright IBM Corp 1990–2006, Copyright MPI fuer Festkoerperforschung Stuttgart 1997–2001, CPMD V3.11.
19. Soler, J. M., Artacho, E., Gale, J. D., García, A., Junquera, J., Ordejón, P. & Sánchez-Portal, D. *J. Phys.: Condens. Matter*, 2002, **14**, 2745.
20. Artacho, E., Anglada, E., Diéguez, O., Gale, J. D., García, A., Junquera, J., Martin, R. M., Ordejón, P., Pruneda, J. M., Sánchez-Portal, D. & Soler, J. M. *J. Phys.: Condens. Matter*, 2008, **20**, 064208.
21. Anglada, E., Soler, J. M., Junquera, J. & Artacho, E. *Phys. Rev. B*, 2002, **66**, 205101.
22. Ferlat, G., Cormier, L., Mauri, F., Balan, E., Charpentier, T., Anglada, E. & Calas, G. *Phys. Chem. Glasses: Eur. J. Glass Sci. Technol. B*, 2006, **47**, 441.
23. Brazhkin, V. V., Katayama, Y., Trachenko, K., Tsiok, O. B., Lyapin, A. G., Artacho, E., Dove, M., Ferlat, G., Inamura, Y. & Saitoh, H. *Phys. Rev. Lett.*, 2008, **101**, 035702.